The Journal of Immunology

Sphingosine 1-Phosphate Lyase Enhances the Activation of IKK ε To Promote Type I IFN–Mediated Innate Immune Responses to Influenza A Virus Infection

Madhuvanthi Vijayan, Chuan Xia, Yul Eum Song, Hanh Ngo, Caleb J. Studstill, Kelly Drews, Todd E. Fox, Marc C. Johnson, John Hiscott, Mark Kester, Stephen Alexander and Bumsuk Hahm

J Immunol 2017; 199:677-687; Prepublished online 9 June 2017;
doi: 10.4049/jimmunol.1601959
http://www.jimmunol.org/content/199/2/677

The Journal of Immunology is published twice each month by
The American Association of Immunologists, Inc.,
1451 Rockville Pike, Suite 650, Rockville, MD 20852

Print ISSN: 0022-1767 Online ISSN: 1550-6606.

Sphingosine 1-Phosphate Lyase Enhances the Activation of IKKε To Promote Type I IFN–Mediated Innate Immune Responses to Influenza A Virus Infection

Madhuvanthi Vijayan,*,† Chuan Xia,*,† Yul Eum Song,† Hanh Ngo,*,† Caleb J. Studstill,*,† Kelly Drews,‡ Todd E. Fox,§ Marc C. Johnson,† John Hiscott,¶ Mark Kester,§ Stephen Alexander,‖ and Bumsuk Hahm*,†

Sphingosine 1-phosphate (S1P) lyase (SPL) is an intracellular enzyme that mediates the irreversible degradation of the bioactive lipid S1P. We have previously reported that overexpressed SPL displays anti-influenza viral activity; however, the underlying mechanism is incompletely understood. In this study, we demonstrate that SPL functions as a positive regulator of IKKε to propel type I IFN–mediated innate immune responses against viral infection. Exogenous SPL expression inhibited influenza A virus replication, which correlated with an increase in type I IFN production and IFN-stimulated gene accumulation upon infection. In contrast, the lack of SPL expression led to an elevated cellular susceptibility to influenza A virus infection. In support of this, SPL-deficient cells were defective in mounting an effective IFN response when stimulated by influenza viral RNAs. SPL augmented the activation status of IKKε and enhanced the kinase-induced phosphorylation of IRF3 and the synthesis of type I IFNs. However, the S1P degradation-incompetent form of SPL also enhanced IFN responses, suggesting that SPL's pro-IFN function is independent of S1P. Biochemical analyses revealed that SPL, as well as the mutant form of SPL, interacts with IKKε. Importantly, when endogenous IKKε was downregulated using a small interfering RNA approach, SPL's anti-influenza viral activity was markedly suppressed. This indicates that IKKε is crucial for SPL-mediated inhibition of influenza virus replication. Thus, the results illustrate the functional significance of the SPL–IKKε–IFN axis during host innate immunity against viral infection. ***The Journal of Immunology*****, 2017, 199: 677–687.**

The type I IFN response is a first line of defense in the innate immune system that protects the host from pathogenic viral infections (1, 2). The potent antiviral activity of type I IFNs, which include 13 isotypes of IFN-α and a single IFN-β, has been observed during infections by numerous viruses, including influenza (3, 4). Influenza virus infection induces type I IFNs upon cellular sensing of viral RNA (vRNA) products, primarily by RIG-I, which recognizes the 5′ppp moiety on influenza vRNAs (5–7). Upon activation of RIG-I, the downstream adaptor protein MAVS is engaged, followed by recruitment of the kinases IKKε and TBK1 (8), both of which can phosphorylate IRF3 and IRF7. Phosphorylated IRF3 and IRF7 act as the major transcription factors that drive the production of IFN-β and IFN-α4, followed by the production of other IFN-α subtypes (9). Binding of IFNs to the cognate receptor (IFNAR) triggers the activation of the JAK–STAT signaling pathway (10), which culminates in the transcriptional induction of an array of IFN-stimulated genes (ISGs), including MX1, ISG15, OAS1, ISG56, and RIG-I. The ISG products act in concert to limit virus replication, launching the antiviral status (11). The importance of the IFN response upon viral infection is emphasized by the fact that many pathogenic viruses have evolved to antagonize the type I IFN signaling pathway to a certain extent (4, 12, 13). However, despite extensive investigation, the regulatory mechanism of the type I IFN production pathway is not fully understood. Therefore, it is important to identify novel cellular factors that regulate type I IFN synthesis and unravel the detailed molecular action mode for type I IFN responses against microbial infections.

Sphingosine 1-phosphate (S1P) lyase (SPL) is an intracellular enzyme that catalyzes the irreversible cleavage of the bioactive lipid S1P at its C2-C3 carbon into by-products (i.e., hexadecenal and phosphoethanolamine) (14, 15). SPL has been reported to be localized to the endoplasmic reticulum (ER) and is also found in the mitochondrial-associated membrane, which is associated with mitochondria and the ER (14, 16, 17). Because S1P is a bioactive lipid (18–20), SPL has been implicated in diverse cellular processes and diseases, such as cancer, immunity, inflammation, and development (21–26). Yet, a direct role for SPL in the context

*Department of Surgery, University of Missouri, Columbia, MO 65212; †Department of Molecular Microbiology and Immunology, University of Missouri, Columbia, MO 65212; ‡Department of Pathology, University of Virginia, Charlottesville, VA 22908; §Department of Pharmacology, University of Virginia, Charlottesville, VA 22908; ¶Istituto Pasteur-Fondazione Cenci Bolognetti, 00161 Rome, Italy; and ‖Division of Biological Sciences, University of Missouri, Columbia, MO 65211

ORCIDs: 0000-0003-2076-6321 (J.H.); 0000-0001-8231-7025 (M.K.).

Received for publication November 17, 2016. Accepted for publication May 12, 2017.

This work was supported by National Institutes of Health/National Institute of Allergy and Infectious Diseases Grant R01AI091797 (to B.H.) and National Institutes of Health Grants R01AI108861 (to J.H.) and GM110776 (to M.C.J.).

Address correspondence and reprint requests to Prof. Bumsuk Hahm, University of Missouri, One Hospital Drive, Medical Sciences Building, NW301C, Columbia, MO 65212. E-mail address: hahmb@health.missouri.edu

The online version of this article contains supplemental material.

Abbreviations used in this article: cRNA, cellular RNA; CTR, empty vector control DNA; dpi, day postinfection; ER, endoplasmic reticulum; HA, hemagglutinin; hpi, hour postinfection; IAV, influenza A virus; IP, immunoprecipitation; ISG, IFN-stimulated gene; KO, knockout; MEF, mouse embryonic fibroblast; MOI, multiplicity of infection; qPCR, quantitative PCR; SCR, Trilencer-27 Universal scrambled negative-control siRNA duplex; si-IKKε, siRNA duplex targeting IKKε; siRNA, small interfering RNA; si-SPL, siRNA duplex targeting SPL; SPL, S1P lyase; S1P, sphingosine 1-phosphate; $S1P_1R$, S1P receptor 1; vRNA, viral RNA; WT, wild-type.

of the innate immune response to virus infections has not been characterized.

We have previously reported that cells constitutively overexpressing SPL were resistant to the replication of influenza A virus (IAV) (27, 28). In this study, we have characterized the contribution of endogenous SPL to the type I IFN production pathway when a pattern recognition receptor, such as RIG-I, is stimulated following virus infection. We found that endogenous SPL is critical for eliciting an effective IFN response upon cellular recognition of influenza vRNAs. More importantly, SPL binds to the kinase IKKε, thereby increasing its activation to promote the synthesis of type I IFN. Collectively, our results demonstrate that SPL is a host factor that augments type I IFN responses during virus infection. Further, this study delineates the relationship between IKKε and SPL, which provides a mechanistic understanding of the pro-IFN activity of SPL.

Materials and Methods

Cell lines and transfection

293T cells and human lung epithelial A549 cells were cultured in DMEM (Life Technologies), as described elsewhere (29, 30). MDCK cells were cultured in MEM Eagle (Mediatech). Cells were cultured in a CO_2 incubator at 37˚C, and all media were supplemented with 10% FBS (HyClone) and penicillin (100 U/ml)/streptomycin (100 μg/ml) (Invitrogen). Lipofectamine 3000 transfection reagent (Invitrogen) was used to transfect plasmid DNA into A549 cells in 24-well plates, at a concentration of 500 ng/ml of the indicated plasmid DNA, following the protocols recommended by the manufacturer. Empty vector plasmids were used to ensure equal total amounts of DNA were being transfected into each sample. Also, equal amounts of transfection reagent were used for all of the samples, including negative controls. For transfection of DNA into 293T cells, LipoD293 transfection reagent (SignaGen Laboratories) was used, according to the manufacturer's instructions, in 24- or 6-well plates. Lipofectamine RNAiMAX was used to perform small interfering RNA (siRNA) transfections on 293T cells in 24-well plates. For SPL-reconstitution experiments, we have used a transient transfection approach to overexpress SPL protein in SPL-deficient cells. SPL-knockout (KO) cells (2×10^5) were transfected with 0.5 μg of SPL or SPL(K353L)-encoding plasmid, and the expression of SPL was confirmed by Western blot analysis.

DNA vector constructs

Mammalian expression plasmids encoding wild-type (WT) SPL constructs, including pc-hSPL and pc-hSPL-GFP, and the enzymatically inactive mutant SPL constructs, including pc-hSPL(K353L) and pc-hSPL(K353L)-GFP, were provided by Julie D. Saba (Children's Hospital Oakland Research Institute, Oakland, CA) (31). The mutation site sequences in the SPL(K353L) constructs were confirmed by DNA sequencing at the DNA core facility (University of Missouri). Mammalian expression plasmids encoding Flag-tagged IKKε, Myc-tagged TBK1, IRF3, Flag-tagged IRF7, and luciferase reporter constructs IFN-α1/pGL3 and IFN-β/pGL3 were used previously (8, 32). To generate the hemagglutinin (HA)-tagged SPL construct, the SPL-coding sequence from pVB003-Flag-hSPL (23) was amplified by PCR using forward primer 5′-CGGAATTCGCCCTAGCACAGACCTTCTGAT-3′ and reverse primer 5′-GGGGTACCTCAGTGGGGTTTTGGAGAAC-3′. The amplified full-length SPL-encoding PCR fragments were treated with EcoRI/KpnI and inserted into an EcoRI/KpnI-digested pCMV-HA vector, which was provided by Dr. David Pintel (University of Missouri). The nucleotide sequences of the subcloned full-length HA-tagged SPL construct were confirmed by DNA sequencing.

Viruses

Influenza A/WSN/33 (H1N1) virus was initially provided by Yoshihiro Kawaoka (University of Wisconsin–Madison, Madison, WI). MDCK epithelial cells were used to amplify the virus. Virus infection and titration studies were performed as described previously (27, 29, 30). For the infection studies, cells were infected with IAV for 1 h and then incubated with the medium. The supernatants containing infectious viruses were harvested for the titration by plaque assay on MDCK cells. For the plaque assay, using serial dilutions of culture supernatants, viruses were adsorbed onto 3×10^5 MDCK cells per milliliter for 1 h and then the cells were incubated with 2× Eagle MEM (Life Technologies) mixed with an equal portion of 1% agarose (SeaKem ME Agarose). Cells were fixed with 25% formalin and stained with Crystal Violet after 2–3 d of incubation to count plaques that are generated by viral cytopathic effects.

CRISPR-Cas9 knockout of SPL

293T stable cell lines knocked out for SPL were generated by transduction with lentiCRISPR v2 (a gift from Feng Zhang, Massachusetts Institute of Technology, Cambridge, MA; Addgene Plasmid 52961) (33). Puromycin selection was performed, followed by single-cell isolation and clonal expansion. Target sequences used as guide RNA sequences were 5′-GGTCCCATTGACGAAGATGATGG-3′ (exon 9) and 5′-GCATCACATTACTACACGCCCGG-3′ (exon 14). To verify disruption of the *SGPL1* gene open reading frame, genomic DNA from the cell lines was extracted and PCR amplified with flanking primers to amplify the target region. Primer sequences used for PCR from genomic DNA are 5′-CCCTCACTGTGGGATCACTTC-3′ and 5′-AACGGCTAGTCAACAGGAGG-3′ for exon 9 and 5′-TGACACCCCAAGCATGAGAG-3′ and 5′-GATGTCTGTGGCAAAGGGGC-3′ for exon 14. Among KO cells, two cell lines were chosen and used in this study based on the loss of SPL protein expression. Exon 9–KO cells (KO-1) used in the study had a deletion of 9 and 27 nucleotides in each chromosome, and exon 14–KO cells (KO-2) had an insertion of 1 and 2 nucleotides in each chromosome.

Western blot analysis and Abs

Western blotting was performed as described elsewhere (27, 29, 30, 34). Cells were lysed using 2× sample buffer containing 2-ME and boiled at 95˚C for 10 min. Equal amounts of protein samples were loaded onto a 12% SDS-PAGE gel, followed by transfer of resolved proteins from the gel to nitrocellulose membranes (Bio-Rad). Membrane-bound Abs were detected using an ECL substrate (Thermo Scientific). Abs against influenza viral NP and M1 were purchased from Abcam; Abs against influenza viral NS1, M2, actin, and SPL were purchased from Santa Cruz Biotechnology; Abs against human GAPDH, ISG56, RIG-I, p-IRF3 (Ser^{396}), IRF3, p-IKKε (Ser^{172}), IKKε, p-TBK1 (Ser^{172}), TBK1, Myc tag, GFP, p-STAT1 (Tyr^{701}), FLAG tag, and HA tag were purchased from Cell Signaling Technology. Ab against influenza H1N1 NS2 was purchased from GenScript. All of the data presented were repeated at least twice with independent experimental settings.

Real-time PCR

Total cellular RNA (cRNA) was extracted using TRI Reagent (Sigma-Aldrich), according to the manufacturer's instructions, and treated with DNase I (Thermo Scientific) to remove contaminating DNA. Isolated RNA was reverse transcribed using random hexamers (Invitrogen) or the forward NP primer for amplifying IAV-NP negative-sense NP RNA or the reverse NP primer for amplifying IAV-NP positive-sense NP RNA. The resulting cDNA was used as a template for real-time quantitative PCR (qPCR) using gene-specific primers. The following primers were used: human MX1 (5′-GTT TCC GAA GTG GAC ATC GCA-3′ and 5′-CTG CAC AGG TTG TTC TCA GC-3′), human ISG15 (5′-CGC AGA TCA CCC AGA AGA TCG-3′ and 5′-TTC GTC GCA TTT GTC CAC CA-3′), human OAS-1 (5′-GAT CTC AGA AAT ACC CCA GCC A-3′ and 5′-AGC TAC CTC GGA AGC ACC TT-3′), human IFN-β (5′-CGC CGC ATT GAC CAT CTA-3′ and 5′-GAC ATT AGC CAG GAG GTT CTC A-3′), and IAV NP (5′-TGC TTC CAA TGA AAA CAT GG-3′ and 5′-GCC CTC TGT TGA TTG GTG TT-3′). qPCR was performed with SYBR Green I chemistry using a StepOnePlus Real-Time PCR System. cDNA quantities were normalized to the corresponding GAPDH RNA quantities from the same samples. All of the data presented were repeated at least twice with independent experimental settings.

Luciferase reporter assay

293T cells (2×10^5) were transfected in 24-well plates with IFN response–triggering plasmids, such as IKKε, IRF3, and IRF7, along with reporter plasmids (50 ng of IFN-β/pGL3 reporter plasmid or IFN-α1/pGL3), as indicated, along with 10 ng of pRL-CMV (Promega) encoding *Renilla* luciferase as a transfection control in the presence of SPL or empty vector control DNA (CTR). At 24 h posttransfection, cells were lysed in the passive lysis buffer to measure *Renilla* and firefly luciferase activities using the Dual-Luciferase Reporter Assay System (Promega), according to the manufacturer's instructions. Luminescence values were measured using a Perkin Elmer EnSpire 2300 multilabel reader.

Coimmunoprecipitation assay

293T (2×10^6) cells in 100-mm tissue culture dishes were transfected with 5 μg of GFP-SPL (a gift from Dr. Julie D. Saba, Children's Hospital Oakland Research Institute) and control vector or 5 μg of Flag-IKKε. One day after transfection, cells were harvested in 1 ml of immunoprecipitation (IP) lysis buffer (Thermo Scientific) containing protease inhibitor mixture and PMSF (1 mM). Cell lysates were incubated with 20 μl of anti-DYKDDDDK G1 affinity resin overnight under rotation at 4°C. For the GFP or Myc pull-down experiment, plain beads were coated with anti-GFP or anti-MYC Ab (Cell Signaling Technology), respectively, and 20 μl of these beads were incubated with cell lysates overnight under rotation at 4°C. For the HA pull-down experiment, 20 μl of anti-HA affinity resin (Pierce) was used for incubation with cell lysates. The beads were washed three times intensively with IP lysis buffer to remove any proteins bound nonspecifically. After the final wash, sample buffer containing 2-ME was added to the beads. The lysates were boiled for 10 min and then used for Western blotting. The experiments were repeated independently at least twice with similar results.

Confocal microscopy

293T cells were plated on four- or eight-well chamber slides (Nunc). The following day, cells were transfected with 200 ng each of the indicated plasmids using LipoD293 transfection reagent (SignaGen Laboratories). At 1 d after transfection, cells were fixed in 4% paraformaldehyde (Fisher Scientific) and then permeabilized in 0.5% Triton X-100 (Sigma-Aldrich) for 10 min at room temperature. Samples were blocked with 10% BSA for 30 min, followed by overnight incubation with the indicated primary Abs, anti-Flag (1:1000) Ab, or anti-GFP Ab (1:100) in 3% BSA overnight at 4°C. After washing, samples were incubated with Alexa Fluor 488–conjugated anti rabbit IgG (1:500) or Alexa Fluor 568–conjugated anti-mouse IgG (1:500) (both from Invitrogen) for 2 h, followed by staining with DRAQ5 dye (300 nM; Thermo Scientific) for 15 min at room temperature. Images were acquired on a Leica SPE2 DM5500Q confocal microscope and analyzed with LSM Image Browser software. Representative fields are shown; each image was selected from 5–10 fields. Results were equivalent in repeated experiments.

RNA interference

A 27mer siRNA duplex targeting IKKε (si-IKKε) and a Trilencer-27 Universal scrambled negative-control siRNA duplex (SCR) were purchased from OriGene and used at a final concentration of 20 nM to transfect 293T cells using Lipofectamine RNAiMAX transfection reagent, according to the manufacturer's instructions. A 27mer siRNA duplex targeting SPL (si-SPL; OriGene) was used at a final concentration of 25 nM to transfect 293T cells. Cells were harvested 2 d post-siRNA transfection, and the knockdown of IKKε and SPL was confirmed by Western blotting.

Statistical analysis

All bars represent means, error bars show SEM, and averages were compared using a bidirectional, unpaired Student *t* test. Data are representative of two or three independent experimental repetitions.

Results

SPL inhibits IAV replication, which is associated with an increased type I IFN response

We have previously observed that SPL overexpression inhibited replication of IAV (27). In that study, we had primarily used the cell line that overexpresses SPL protein constitutively. To determine whether the long-term constant expression of SPL is essential for the suppression of viral replication, a transient transfection experiment was performed. As shown in Fig. 1A, transient overexpression of SPL inhibited the expression of IAV proteins, such as NS1 and M2, at an multiplicity of infection (MOI) of 1 and 3. The result suggests that SPL exhibits antiviral activity regardless of whether SPL is temporarily or stably overexpressed. To further determine the role of endogenous SPL in viral replication, SPL-deficient cells were created using the CRISPR/Cas9-mediated genetic approach, as described in *Materials and Methods* (33). We selected two cell lines based on the knockout of endogenous SPL, as confirmed by Western blot analysis (Fig. 1B, 1C). SPL-deficient cells (KO-1 and KO-2 cells) proliferated at a similar rate compared with SPL-sufficient WT cells, without any noticeable defects in cell growth (Supplemental Fig. 1). Upon IAV infection, KO-1 and KO-2 cells exhibited an enhanced susceptibility to IAV replication, as shown by a strong increase in the level of structural and nonstructural

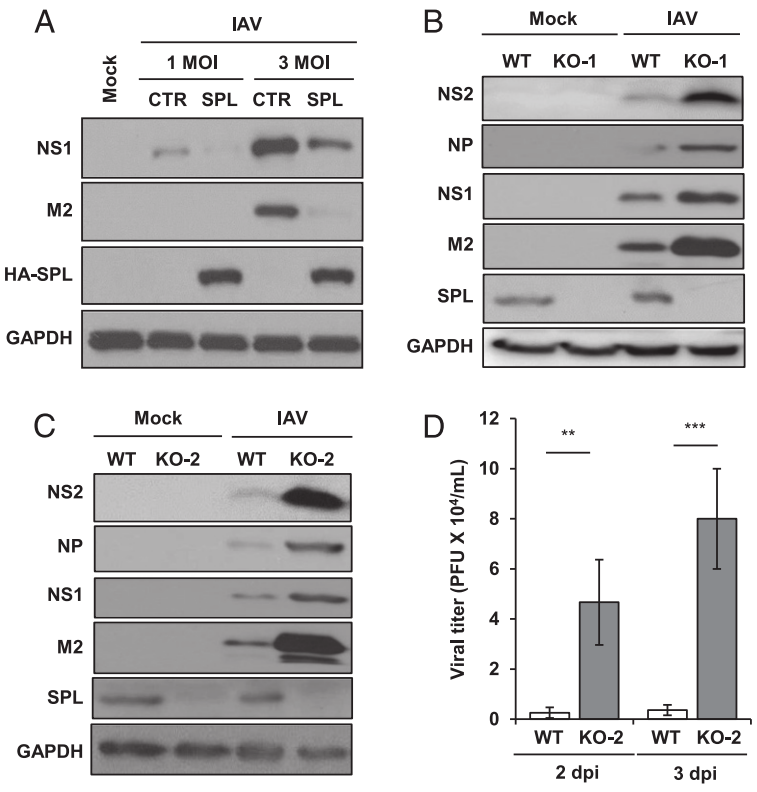

FIGURE 1. SPL inhibits the replication of influenza virus. (**A**) A549 cells (2×10^5) were transfected with CTR or HA-tagged SPL (HA-SPL)-encoding DNA. One day later, cells were mock infected (Mock) or were infected with IAV at an MOI of 1 or 3. At 8 hpi, cells were harvested for Western blot analysis to check the levels of NS1, M2, HA-SPL, and GAPDH. WT, KO-1 cells (**B**), and KO-2 cells (1×10^6) (**C**) were infected with IAV at an MOI of 0.1 or were mock infected. At 1 dpi, Western blotting was performed to detect NS2, NP, NS1, M2, SPL, and GAPDH proteins. (**D**) WT or KO-2 cells (2×10^5) were infected with IAV at an MOI of 0.01. A plaque assay was performed at 2 and 3 dpi to determine viral titer in the supernatant of the infected cells. Data represent mean ± SEM ($n = 3$ per group). $^{**}p \leq 0.01$, $^{***}p \leq 0.001$.

IAV proteins, such as NS2, NP, NS1, and M2 (Fig. 1B, 1C). Furthermore, we investigated the role of endogenous SPL in IAV propagation by comparing the production of infectious IAV from WT or SPL-deficient cells. As shown in Fig. 1D, the lack of endogenous SPL significantly increased IAV production at 2 and 3 d postinfection (dpi). These data further verify the antiviral function of endogenous SPL.

Type I IFNs are the major antiviral cytokines produced by virus-infected cells, and the SPL-overexpressing cell line appeared to exhibit enhanced IFN signaling to repress IAV replication (27, 35). We further assessed the effect of SPL expression on type I IFN responses to IAV infection. Transient overexpression of SPL led to a significant increase in IFN-β production at 4 h postinfection (hpi) when measured by qPCR (Fig. 2A). However, at 6 hpi, little increase was observed in SPL-overexpressing cells compared with the control vector–transfected infected cells, suggesting a temporal increase in IFN synthesis by SPL. Because ISGs are the ultimate antiviral effectors of the type I IFN response, we measured the extent of ISG upregulation. SPL enhanced the mRNA level of MX1 by ∼2-fold (Fig. 2B). Also, SPL overexpression modestly enhanced the protein level of ISGs, such as RIG-I and ISG56 (Fig. 2C). These ISGs have been reported to play important antiviral roles during influenza virus infection (36, 37). Of note, in the mock-infected cells, SPL alone did not induce IFN responses,

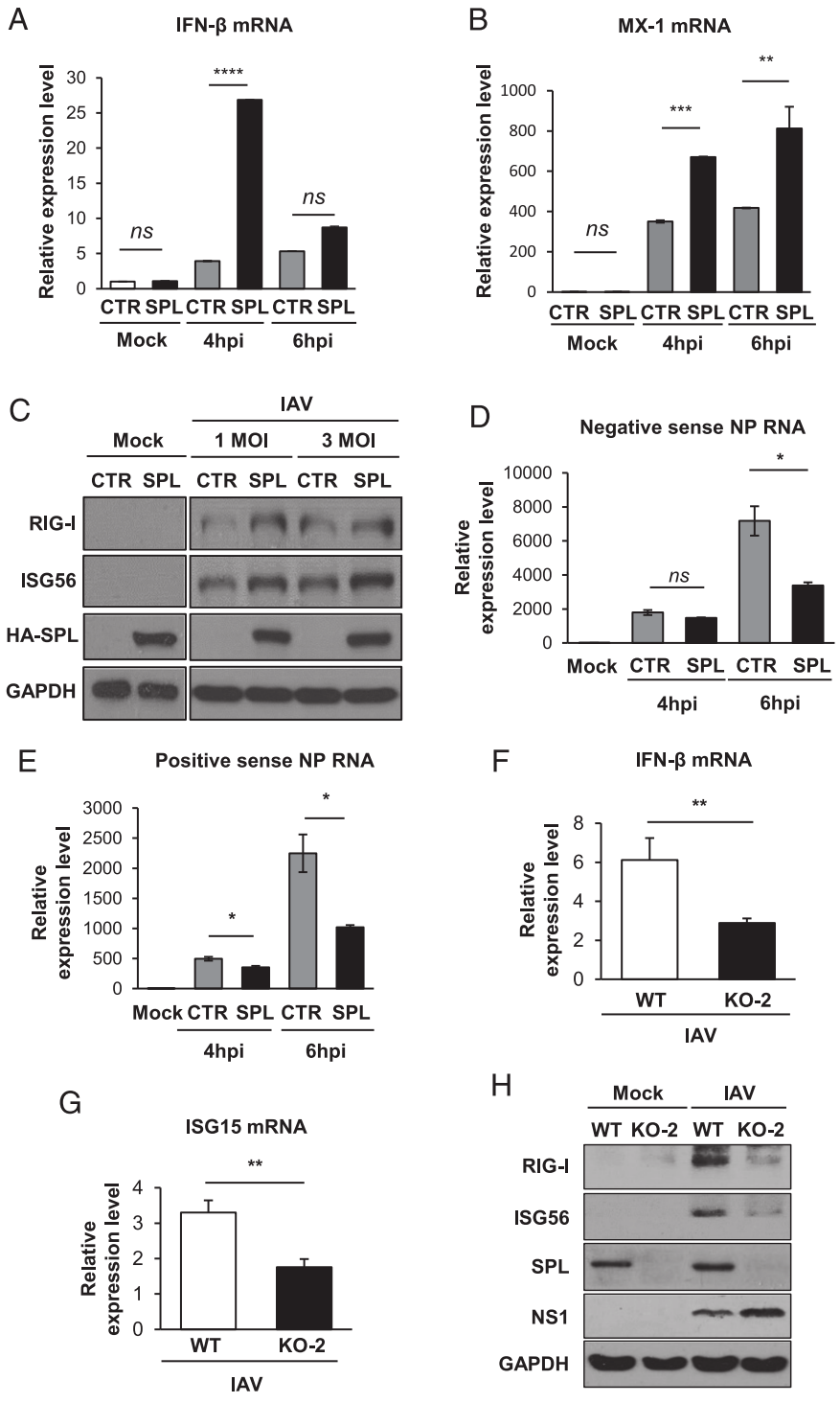

FIGURE 2. SPL increases the type I IFN response to influenza virus infection. (**A** and **B**) A549 cells (2×10^5) were transfected with CTR or SPL. At 1 d posttransfection, cells were mock infected or were infected with IAV at an MOI of 0.5. Relative RNA levels of IFN-β (A) and MX1 (B) were calculated by qPCR at 4 and 6 hpi. Data represent mean ± SEM ($n = 3$ per group). (**C**) A549 cells (2×10^5) were transfected with CTR or HA-tagged SPL (HA-SPL)-encoding DNA. One day later, cells were mock infected (Mock) or were infected with IAV at an MOI of 1 or 3. At 8 hpi, cells were harvested for Western blot analysis to check the levels of RIG-I, ISG56, HA-SPL, and GAPDH proteins. (**D** and **E**) A549 cells (2×10^5) were transfected with CTR or SPL. At 1 d posttransfection, cells were mock infected or were infected with IAV at an MOI of 0.5. Relative levels of IAV NP negative-sense RNA (D) and IAV NP positive-sense RNA (E) were calculated by qPCR at 4 and 6 hpi. Data represent mean ± SEM ($n = 3$ per group). (**F**) WT 293T cells or KO-2 cells (2×10^5) were mock infected or were infected with IAV at an MOI of 0.01. At 2 dpi, the relative levels of IFN-β (F) and ISG15 (**G**) were calculated by qPCR. Data represent mean ± SEM ($n = 3$ per group). (**H**) WT 293T cells or KO-2 cells (2×10^5) were mock infected or were infected with IAV at an MOI of 0.01. At 2 dpi, cells were harvested for Western blot analysis to check the levels of RIG-I, ISG56, SPL, NS1, and GAPDH proteins. $*p \le 0.05$, $**p \le 0.01$, $***p \le 0.001$, $****p \le 0.0001$. *ns*, not significant.

suggesting that SPL functions as a pro-IFN factor after cellular sensing of viral infection (Fig. 2A–C). Accordingly, SPL was shown to suppress the synthesis of viral NP-specific RNAs of positive- and negative-sense RNAs at 6 hpi (Fig. 2D, 2E). The transient increase in IFN production by SPL at 4 hpi, followed by its rapid decrease at 6 hpi (Fig. 2A), could be due to the lower amounts of IFN-stimulatory vRNAs present in SPL-overexpressing cells compared with control cells (Fig. 2D, 2E). Further, we have examined the type I IFN response during IAV infection in SPL-deficient cells. Following IAV infection, endogenous SPL was shown to be critical for the effective production of IFN-β (Fig. 2F) and ISGs, such as ISG15 (Fig. 2G) and RIG-I and ISG56 (Fig. 2H). Collectively, these data demonstrate that SPL augments type I IFN and ISG production, which correlates with a decrease in IAV replication.

Endogenous SPL is important for efficient induction of IFN responses upon cellular sensing of influenza vRNAs

Although SPL enhanced IFN responses during IAV infection, the effect appeared to be modest (Fig. 2B, 2C). This could be due to the presence of a dynamic antagonistic interaction between viral components and host cellular factors of the IFN system during the IAV-replication process (30, 38–44). To overcome this, we opted for a method to trigger an IFN response other than IAV infection. Hence, vRNAs that were purified from IAV-infected cells were used to stimulate IFN production. Transfection of cells with influenza vRNAs was reported to activate the RIG-I signaling pathway by recognition of triphosphate moieties on the vRNAs, leading to an induction of type I IFNs (5–7, 45). cRNAs were isolated from uninfected cells and used as a negative control. Following transfection with vRNAs, cells deficient in endogenous SPL (KO-1 and KO-2 cells) were much less efficient at synthesizing IFN-β mRNA than were SPL-sufficient WT cells (Fig. 3A). The decreased production of IFNs caused by SPL deficiency resulted in the decreased upregulation of ISG-specific mRNAs, such as ISG15 (Fig. 3B) and OAS1 (Fig. 3C). Accordingly, SPL deficiency markedly suppressed the protein expression of ISGs such as RIG-I and ISG56 (Fig. 3D, 3E). Consistent with these findings, when SPL was downregulated by an siRNA, vRNA-induced expression of RIG-I and ISG56 was impaired (Fig. 3F). These data clearly demonstrate that endogenous SPL is important for efficient production of type I IFNs and ISG products, which, in turn, may establish optimal antiviral conditions upon cellular recognition of IAV RNAs.

SPL interacts with IKKε and augments IKKε activation that leads to enhanced type I IFN production

IKKε and TBK1 phosphorylate and activate IRF3, which functions as a transcription factor to direct type I IFN synthesis (8, 9). To define the molecular mechanism behind SPL's pro-IFN activity, we investigated whether SPL regulates IKKε or TBK1 activation, which leads to the activation of IRF3. Although TBK1 was autophosphorylated and induced IRF3 phosphorylation, SPL had no effect on the level of TBK1 autophosphorylation or TBK1-mediated IRF3 phosphorylation (Supplemental Fig. 2A), suggesting that SPL does not affect TBK1-mediated IFN responses. In contrast, SPL increased the level of the activated form of IKKε (p-IKKε at Ser^{172}) and IKKε-mediated phosphorylation of IRF3 (Fig. 4A). Further, SPL increased the level of p-IKKε in a dose-dependent manner (Fig. 4B). These data indicate that SPL promotes the activation of IKKε but not that of TBK1. To further investigate whether SPL regulates IKKε activation, we used the luciferase reporter assay to measure the promoter activities of IFN-α/β. This allows us to determine whether SPL has the ability to influence IKKε-induced IFN synthesis. As shown in Fig. 4C, SPL significantly increased IKKε-mediated activation of the

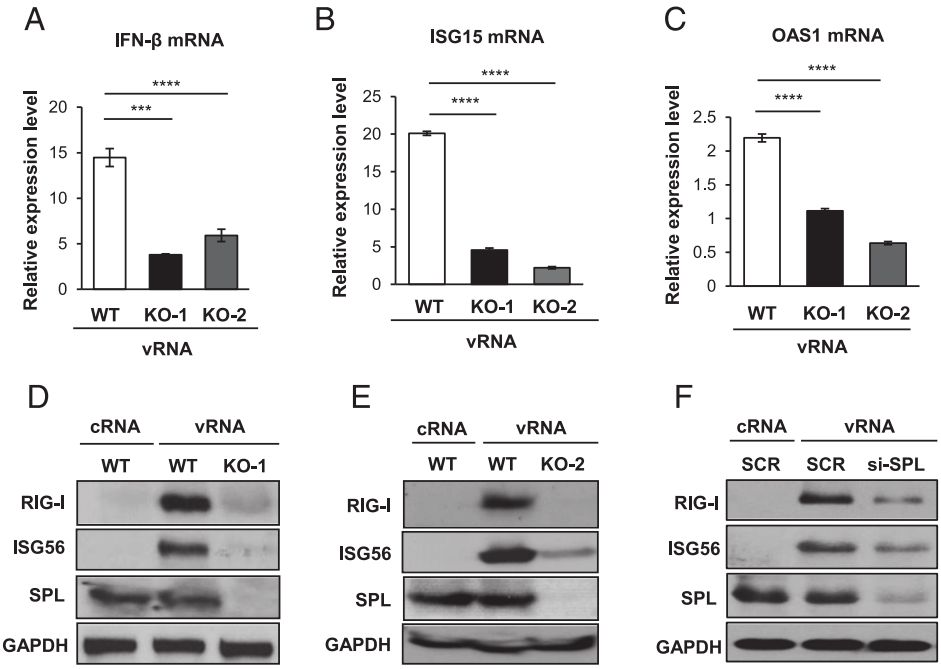

FIGURE 3. SPL is important for mounting an effective IFN response upon cellular recognition of influenza vRNAs. (**A**–**C**) WT 293T cells, KO-1 cells, or KO-2 cells (1×10^6) were transfected with RNAs isolated from IAV-infected cells (vRNAs) or RNAs isolated from noninfected cells (cRNAs) at a concentration of 2.5 μg/ml. At 1 d after transfection, relative mRNA levels of IFN-β (A), ISG15 (B), and OAS1 (C) were determined by performing qPCR and plotted as fold induction over cRNA-treated samples. Data represent mean ± SEM ($n = 3$ per group). WT 293T cells, KO-1 cells (**D**), and KO-2 cells (1×10^6) (**E**) were transfected with vRNA or cRNA. After 1 d, Western blotting was performed to detect RIG-I, ISG56, SPL, and GAPDH proteins. (**F**) 293T cells were transfected with si-SPL or SCR. At 24 h posttransfection, cells were transfected with vRNA or cRNA at a concentration of 1.25 μg/ml. One day later, the levels of RIG-I, ISG56, SPL, and GAPDH were analyzed by Western blotting. ***$p \leq 0.001$, ****$p \leq 0.0001$.

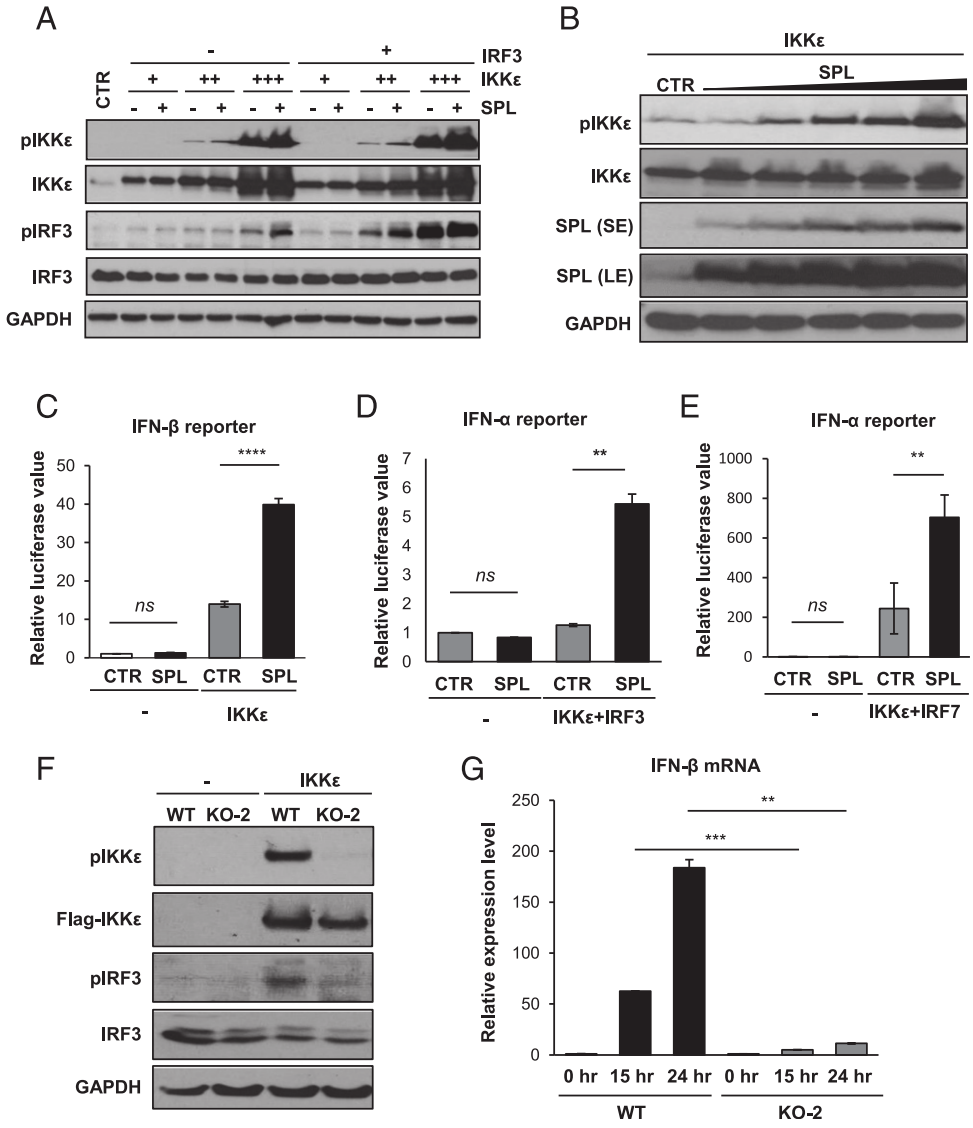

FIGURE 4. SPL increases IKKε activation to enhance IKKε-mediated IFN induction. (**A**) 293T cells (2×10^5) were transfected with increasing doses of IKKε expression plasmid (+, 5 ng; ++, 25 ng; +++, 125 ng) in the presence of 200 ng of IRF3 plasmid or empty vector control plasmid (−) in the presence of 200 ng of SPL plasmid or the empty vector control plasmid (−), as indicated. After 10 h, cells were harvested, and Western blotting was performed to detect p-IKKε, IKKε, p-IRF3, IRF3, and GAPDH. (**B**) 293T cells (1×10^6) were transfected with 25 ng of IKKε with increasing doses of SPL plasmid (0.2, 0.4, 0.6, 0.8, or 1 μg). Ten hour later, Western blot analysis was performed to detect p-IKKε, IKKε, SPL, or GAPDH. The short-exposure (SE) and long-exposure (LE) blots of SPL are shown. (**C**) 293T cells were transfected with 50 ng of IFN-β reporter plasmid along with 10 ng of IKKε plasmid in the presence of SPL or CTR. At 1 d posttransfection, luciferase assay was performed. 293T cells were transfected with 100 ng of IFN-α1 reporter plasmid along with 10 ng of IKKε and IRF3 (**D**) or 10 ng of IKKε and IRF7 (**E**), in the presence of 250 ng of SPL or CTR. At 1 d posttransfection, cells were harvested, and luciferase assay was performed. Relative luciferase values are shown. Data represent mean ± SEM ($n = 3$ per group). (**F**) WT 293T cells or SPL KO-2 cells (2×10^5) were transfected with 50 ng of IKKε expression plasmid or empty vector control plasmid (-). Thirty-two hours later, Western blot analysis was performed to detect p-IKKε, IKKε, p-IRF3, IRF3, and GAPDH. (**G**) WT 293T cells or SPL KO-2 cells (2×10^5) were transfected with 50 ng of IKKε expression plasmid or empty vector control plasmid (0 h). Twenty-four hours later, relative mRNA levels of IFN-β were determined by qPCR. Results are plotted as fold induction of IFN-β in WT and KO-2 samples over the value from each sample transfected with empty vector control plasmid (0 h). Data represent mean ± SEM ($n = 3$ per group). $^{**}p \leq 0.01$, $^{***}p \leq 0.001$, $^{****}p \leq 0.0001$. *ns*, not significant.

IFN-β promoter. Also, SPL promoted IKKε-mediated activation of the IFN-α promoter compared with the control when stimulated along with IRF3 (Fig. 4D) or IRF7 (Fig. 4E). However, SPL overexpression in the absence of IKKε was not capable of inducing transcriptional activation of type I IFN (Fig. 4C–E). We have further investigated SPL's function in promoting IKKε activation by using SPL-deficient cells. As shown in Fig. 4F, SPL deficiency resulted in the strong inhibition of IKKε autophosphorylation. Consistently, we have also observed a decrease in IRF3 phosphorylation (Fig. 4F) and IFN-β production (Fig. 4G) in the absence of endogenous SPL. Taken together, these findings indicate that SPL enhances the stimulation of IKKε, leading to the increased activation of transcription factors IRF3 and IRF7 that ultimately enhance the synthesis of IFN-α/β.

To further explore the mode of action behind SPL-mediated IKKε activation, we tested the possible interaction between SPL and IKKε. Co-IP was performed whereby IKKε was pulled down, and the ability of SPL to coprecipitate in the IP fraction was assessed. The data shown in Fig. 5A demonstrated that GFP-tagged SPL interacted with IKKε, whereas GFP itself did not bind to IKKε. The interaction between SPL and IKKε was confirmed by performing the reverse co-IP (i.e., pulling down of SPL,

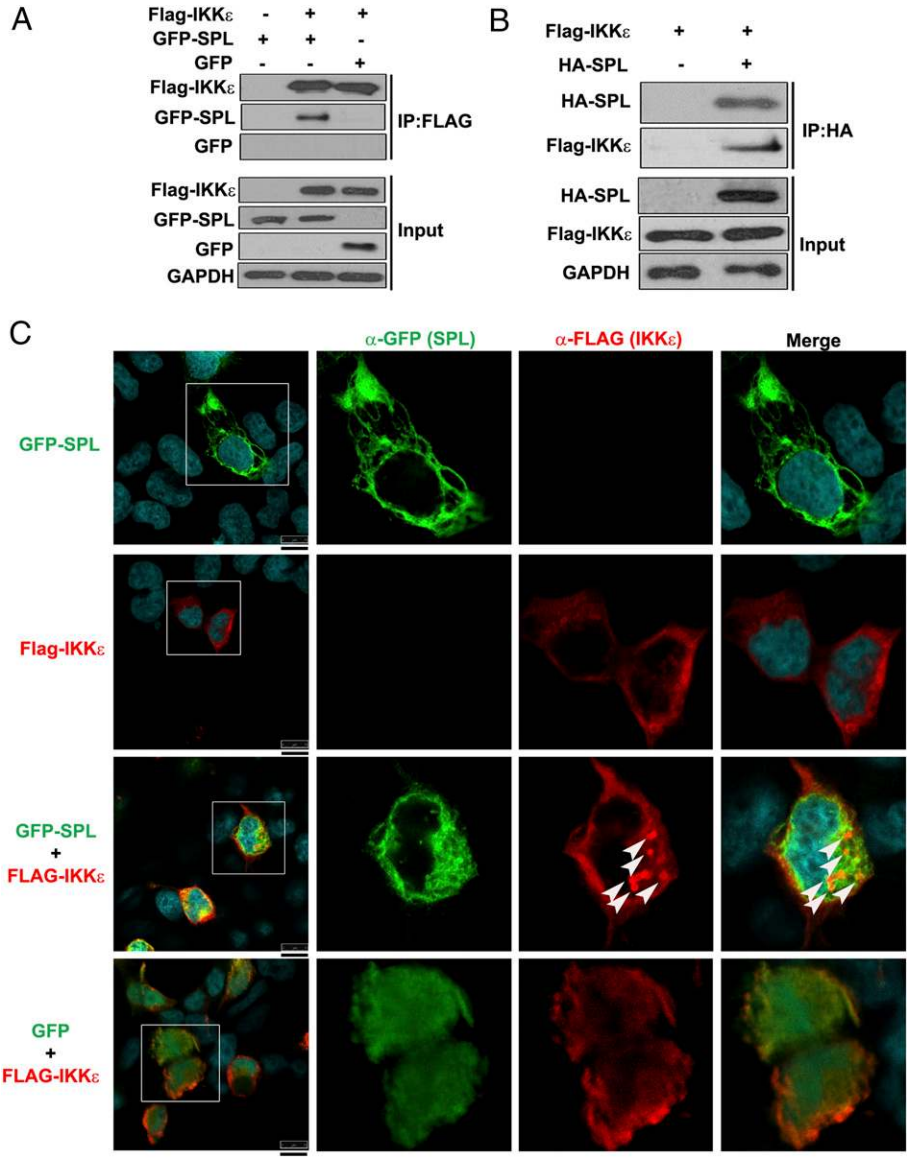

FIGURE 5. SPL interacts with IKKε. (**A**) 293T cells were transfected with Flag-tagged IKKε (Flag-IKKε) in the presence of GFP-tagged SPL (GFP-SPL) or GFP-expressing plasmid (GFP), or an empty control Flag vector (−). Twenty-four hours after transfection, co-IP was carried out using anti-FLAG affinity resin, and Western blotting was performed to detect Flag-IKKε, GFP-SPL, and GFP in the pull-down fractions (IP:FLAG) and in the whole-cell lysates (Input). (**B**) 293T cells were transfected with Flag-IKKε in the presence of an empty control vector (−) or HA-SPL. After 24 h, co-IP was carried out using anti-HA–coated affinity resin. Western blotting was conducted to detect Flag-IKKε and HA-SPL in the pull-down fraction (IP: HA), as well as in the whole-cell lysates (Input). (**C**) Flag-IKKε and GFP-SPL were transfected alone or cotransfected into 293T cells. Flag-IKKε and GFP-expressing plasmid (GFP) were cotransfected into cells (GFP + Flag-IKKε) as a negative control. At 24 h posttransfection, cells were stained with DRAQ5 to detect nuclei, which are shown in the merged images, and with Ab against Flag (α-Flag) to detect IKKε and with Ab against GFP (α-GFP) to detect SPL by confocal microscopy. The boxes in the far left panels are enlarged to show details. Arrowheads indicate the punctate-like structure. Representative confocal images are shown. Scale bars, 10 μm.

followed by detection of IKKε in the immunoprecipitated fraction) (Fig. 5B). However, SPL did not bind to the closely related kinase TBK1 (Supplemental Fig. 2B, 2C). Furthermore, we used confocal microscopy to visualize the localization patterns of SPL and IKKε. SPL has been reported to be localized to cytoplasmic organelles, such as the ER (17, 31). IKKε displayed a diffuse localization pattern throughout the cytoplasm (Fig. 5C, Flag-IKKε). Interestingly, when SPL and IKKε were coexpressed, a substantial fraction of IKKε was redistributed into punctate structures in the cytosol where SPL was colocalized (Fig 5C, GFP-SPL + Flag-IKKε). However, IKKε did not undergo this type of redistribution when coexpressed with GFP (Fig. 5C, GFP + Flag-IKKε), which was used as a negative control. These results led us to conclude that SPL interacts with IKKε, which could facilitate IKKε activation by increasing the phosphorylation status of IKKε. Because we have used the GFP-SPL fusion protein in the aforementioned biochemical assays of co-IP and confocal microscopy, we have also tested the function of GFP-SPL to ensure that GFP-SPL remains functional and displays the same phenotype as the untagged SPL. GFP-SPL was proven to enhance the autophosphorylation of IKKε, similar to the untagged SPL, whereas GFP protein did not affect IKKε phosphorylation (Fig. 6A). In support of this observation, GFP-SPL, but not GFP, increased IFN-β production upon IAV infection (Fig. 6B).

IKKε is important for the antiviral effect exhibited by SPL upon IAV infection

Next, we attempted to ascertain the functional relevance of the SPL–IKKε axis during IAV infection. For this purpose, we downregulated endogenous IKKε, using an siRNA approach in the presence or absence of SPL, upon IAV infection. As expected, SPL displayed an antiviral effect in SCR-treated cells (Fig. 7A) and inhibited the synthesis of viral proteins M1 and NP. However, this antiviral effect of SPL was nearly abrogated when endogenous IKKε was knocked down (Fig. 7A). This observation signifies the importance of IKKε in mediating the antiviral effect exhibited by SPL. To further confirm whether a similar effect is also seen in the production of infectious viruses, we performed a plaque assay using the supernatant from infected cells. In support of the results based on the viral protein expression, downregulation of IKKε nullified SPL's ability to repress infectious IAV production (Fig. 7B). Furthermore, we have repeated the IKKε-knockdown experiment

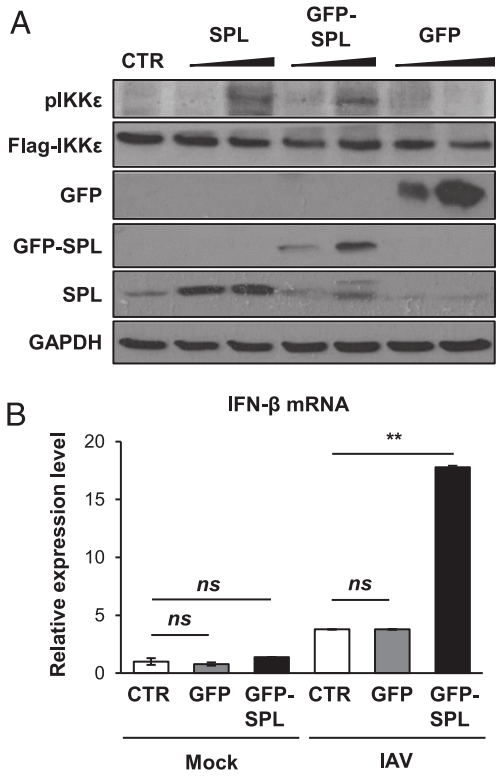

FIGURE 6. GFP fusion does not impair the function of SPL in enhancing IKKε activation and IFN production. (**A**) 293T cells (1×10^6) were transfected with 25 ng of IKKε in the presence of 0.2 or 0.8 μg of SPL plasmid (SPL), GFP-tagged SPL plasmid (GFP-SPL), or GFP-expressing plasmid (GFP). Ten hours later, Western blot analysis was performed to detect p-IKKε, Flag-IKKε, SPL, GFP, and GAPDH. (**B**) A549 cells (2×10^5) were transfected with CTR, GFP, or GFP-SPL. At 1 d posttransfection, cells were mock infected or were infected with IAV at an MOI of 0.5. Relative RNA levels of IFN-β were calculated by qPCR at 6 hpi. Data represent mean ± SEM ($n = 3$ per group). $^{**}p \leq 0.01$. *ns*, not significant.

using A549 cells to confirm our results. SPL's antiviral effect was also abolished when endogenous IKKε was knocked down in A549 cells (Fig. 7C). Additionally, SPL was found to induce the phosphorylation of IKKε at 6 hpi, which must have contributed to SPL's antiviral function. When IKKε was downregulated using siRNA, this phosphorylated fraction of IKKε did not appear (Fig. 7C), which supports the result that SPL acts on IKKε activation to inhibit IAV replication. Taken together, our data further demonstrate that SPL's antiviral activity is dependent on IKKε.

SPL enhances type I IFN responses independent of its enzymatic activity

The enzymatic function of SPL is to degrade intracellular S1P. Hence, we investigated whether the S1P-metabolizing activity of SPL is needed for SPL to exert its pro-IFN function. To examine that, we used the mutant form of SPL, SPL(K353L), which cannot degrade S1P because of a point mutation in its cofactor binding site (31), in our experiments. Interestingly, SPL(K353L) displayed a similar antiviral activity as WT SPL to inhibit IAV replication in SPL-deficient cells (Fig. 8A). Thus, SPL's ability to impair IAV replication seems to be independent of its ability to degrade intracellular S1P. Next, we investigated whether the mutant SPL is capable of increasing IKKε stimulation. As shown in Fig. 8B, SPL(K353L) can increase IKKε activation in a dose-dependent manner, similar to WT SPL (Fig. 4B). In line with these data, co-IP experiments revealed that mutant SPL can also bind to IKKε (Fig. 8C, 8D). These data collectively indicate that SPL acts as a pro-IFN

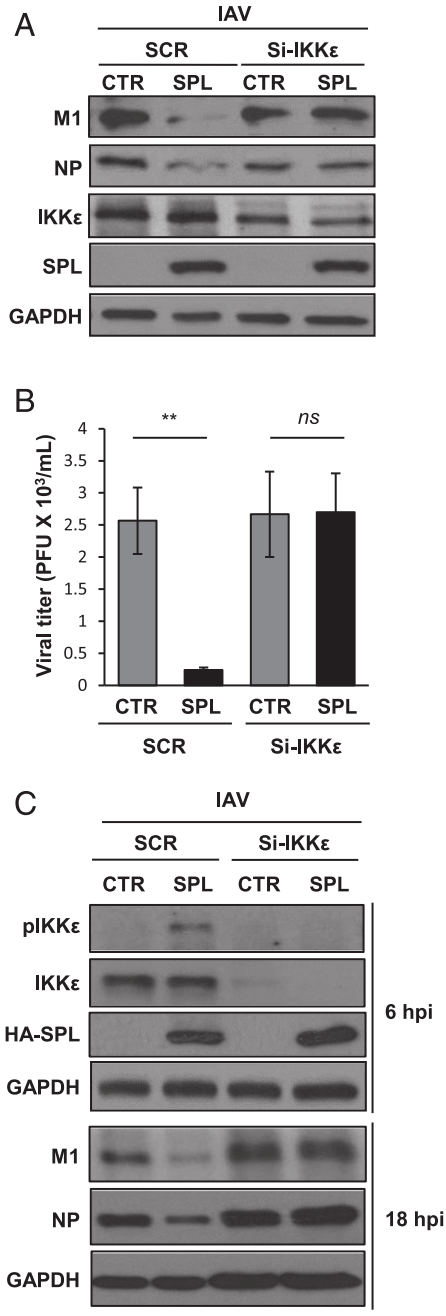

FIGURE 7. IKKε is critical for the antiviral function of SPL during IAV infection. (**A**) SPL KO-1 cells (2×10^5) were transfected with si-IKKε or SCR in the presence of SPL or CTR. Transfected cells were infected with IAV at an MOI of 0.1. At 1 dpi, Western blotting was performed to detect M1, NP, IKKε, HA-SPL, and GAPDH. (**B**) KO-2 cells (2×10^5) were transfected with si-IKKε or SCR in the presence of SPL or CTR. Transfected cells were infected with IAV at an MOI of 0.1. At 24 hpi, the supernatants from MDCK cells were collected to quantify viral titers by plaque assay. Three separate samples of virus-infected cells per group were used for each condition. Data are mean ± SEM ($n = 3$ per group). (**C**) A549 cells (2×10^5) were transfected with si-IKKε or SCR in the presence of SPL or CTR. Transfected cells were infected with IAV at an MOI of 0.5. At 6 hpi, Western blotting was performed to detect p-IKKε, IKKε, HA-SPL, and GAPDH; at 18 hpi, Western blotting was performed to detect viral M1, NP, and GAPDH. $^{**}p \leq 0.01$. *ns*, not significant.

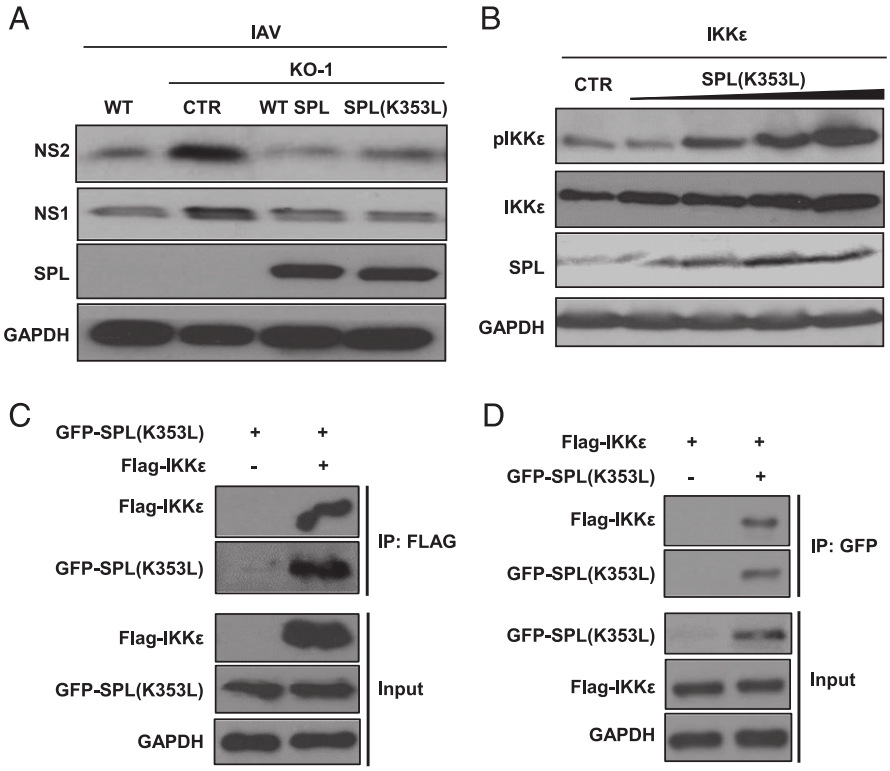

FIGURE 8. SPL enhances the type I IFN response independent of its enzymatic activity. (**A**) WT 293T cells or KO-1 cells (2×10^5) were transfected with CTR, WT SPL, or mutant SPL [SPL(K353L)], as indicated. One day later, transfected cells were infected with IAV at an MOI of 0.1. Western blotting was performed at 1 dpi to detect NS2, NS1, SPL, and GAPDH proteins. (**B**) 293T cells (1×10^6) were transfected with 25 ng of Flag-tagged IKKε with increasing doses (0.4, 0.6, 0.8, or 1 μg) of SPL(K353L) plasmid. Ten hours posttransfection, Western blotting was performed to detect p-IKKε, IKKε, SPL, and GAPDH proteins. (**C**) 293T cells were transfected with GFP-tagged SPL(K353L) [GFP-SPL(K353L)] and either an empty control Flag vector (−) or Flag-tagged IKKε (Flag-IKKε). Twenty-four hours after transfection, IP was carried out using anti-FLAG affinity resin, and Western blotting was performed to detect Flag-IKKε and GFP-SPL(K353L) in the pull-down fractions (IP: FLAG) and in the whole-cell lysates (Input). (**D**) 293T cells were transfected with Flag-IKKε in the presence of an empty control vector (-) or GFP-SPL(K535L). After 24 h, co-IP was carried out using anti-GFP–coated affinity resin. Western blotting was conducted to detect Flag-IKKε and GFP-SPL(K353L) in the pull-down fraction (IP: GFP), as well as in the whole-cell lysates (Input).

factor independent of its enzymatic activity of degrading cellular S1P.

Discussion

In this study, we demonstrate that SPL is critical for host innate immunity by promoting efficient type I IFN responses and establishment of an antiviral state. Mechanistically, SPL augments IFN production by binding and activating the kinase IKKε that phosphorylates IRF3. We delineate the relationship between SPL and IKKε and their interplay to promote IFN-α/β production.

IKKε and TBK1 are known to activate the transcription factors IRF3/IRF7 to induce type I IFNs (8). However, the commonality and differences between these two kinases with regard to their activity in the IFN production pathway are incompletely understood. Although TBK1 is constitutively expressed in most cell types, IKKε is more predominantly detected in immune cells, and its expression is often upregulated upon stimulation with LPS or inflammatory cytokines (46). Also, studies performed with TBK1-deficient and IKKε-deficient mouse embryonic fibroblasts (MEFs) have established a redundant role for IKKε and TBK1 in the IFN response upon polyinosinic-polycytidylic acid treatment, whereas IKKε had a dispensable role in IFN production upon LPS treatment (47). Interestingly, TBK1-deficient MEFs could still mount an IFN response to polyinosinic-polycytidylic acid treatment, which was abolished in IKKε$^{-/-}$ TBK1$^{-/-}$ double-deficient MEFs, indicating that IKKε does play a definitive role in IFN production (47). Thus, the function of IKKε may be more reliant on the type of stimulus or cellular condition. Our findings show that SPL regulates IKKε but not TBK1. The differential effect that SPL has on TBK1 and IKKε activation is further substantiated by our co-IP data, which provide mechanistic evidence that SPL does bind to IKKε but not to TBK1. Determining the in-depth mechanism for the SPL-mediated specific regulation of IKKε may extend our understanding of the differential functions of IKKε and TBK1 in directing the synthesis of type I IFNs.

In the confocal microscopy analysis, we have observed that IKKε relocalizes into punctate cytoplasmic bodies (Fig. 5C). The nature of these cytoplasmic bodies remains unknown. The punctate-like structure of IKKε was also observed when IKKε was coexpressed with another IKKε-binding protein, TRIM6 (48). It was proposed that IKKε relocalizes into TRIM6-ubiquitin–rich bodies for enhanced IKKε activation. Therefore, it is likely that IKKε gathers to form the punctate-like structure when it binds to other cellular proteins for activation of IFN signaling. Whether TRIM6 is involved in SPL-mediated regulation of IKKε activity and/or localization will be interesting to investigate. Also, it remains unknown what triggers SPL to interact with IKKε. We have observed that the SPL expression level does not change upon stimulation by IFN. However, there is a possibility that, upon cellular sensing of vRNAs, SPL undergoes posttranslational modification. Once modified, SPL may exert its function as a pro-IFN factor by interacting with IKKε. Alternatively, upon cellular recognition of vRNAs, activated IKKε may recruit SPL into the IFN pathway. These possibilities are currently under investigation.

Influenza virus was reported to strive to counterattack the potent antiviral IFN response (49, 50). For instance, influenza viral NS1 was shown to antagonize the type I IFN system in multiple ways (6, 49). However, it remains unknown whether IAV proteins, such as NS1, regulate SPL's pro-IFN function or whether SPL modulates the viral protein's anti-IFN effect. Delineating the molecular mechanism behind this dynamic regulation will help us to understand IAV–host interaction pathways.

IKKε$^{-/-}$ mice were hypersusceptible to influenza infection, with increased virus titers in the lungs compared with WT control mice (51). Also, respiratory syncytial virus and vesicular stomatitis virus were shown to induce IKKε expression and/or activation, which contributed to IRF3 activation in response to these infections (52, 53). Furthermore, Ebola virus VP35 protein and nucleoprotein of lymphocytic choriomeningitis virus were reported to interact with IKKε to prevent it from binding to IRF3, thereby antagonizing the cellular IFN response (54, 55). Thus, IKKε is a key player for eliciting the innate immune response in the context of multiple virus infections. By using the IKKε-knockdown approach, we conclusively demonstrated the importance of IKKε in SPL-mediated anti-influenza viral action (Fig. 7). Our study linking SPL to IKKε and the type I IFN response can be extrapolated to other pathogenic virus infections for which the significance of IKKε in the virus lifecycle has already been established.

Our data suggest that the mutant SPL can exhibit antiviral potential to the same extent as WT SPL during IAV infection. These data indicate that the S1P-degrading activity of SPL is not necessary for it to exert its pro-IFN function. This is consistent with the prior observation that sphingosine analogs or S1P receptor 1 ($S1P_1R$) agonist did not affect replication of the influenza virus in vitro and in vivo (27, 28, 56–58). The protein–protein interaction between SPL and IKKε appears to be important and sufficient for SPL to increase IKKε activation to promote the type I IFN response. However, the sphingosine analogs or $S1P_1R$ agonist could regulate cytokine responses during influenza virus infection (56–59). Also, it was recently reported that the agonist of $S1P_1R$ or exogenous S1P can directly induce degradation of type I IFN receptor (IFNAR) to inhibit IFN amplification on plasmacytoid dendritic cells (60). This could be an important mechanism for regulation of the inflammatory response, given that S1P has been shown to affect cytokine/chemokine responses in diverse conditions (61–63). Conceivably, SPL may cause degradation of S1P to prevent $S1P_1R$-mediated IFNAR1 degradation, thereby leading to preservation of an intact IFN pathway. However, the regulation of intracellular SPL may result in altered physiological conditions different from exogenous stimulation of $S1P_1R$. Further, our data indicate that the phenotypic and functional interaction between SPL and IKKε does not require SPL's enzymatic activity. Perhaps cellular detection of vRNAs guides the action of SPL into IKKε-mediated type I IFN pathway in the virus-infected cells. Thus, it is conceivable that SPL has a dual role in regulating host immune responses via S1P-dependent and S1P-independent mechanisms. The intricate mechanisms for sphingolipid system–host immunity interactions need to be investigated further using diverse systems, including the regulation of S1P-metabolizing enzymes, as well as S1PR activation.

It was reported that SPL-KO mice do not survive for more than 2–3 wk after birth (64). More recently, conditional SPL-KO mice have been developed that can be used to study the cell type–specific function of SPL in vivo (65). Investigating the function of SPL in the mice model will allow us to determine the importance of SPL during IAV infection in vivo. Furthermore, the role of SPL in primary human respiratory epithelial cells or immune cells remains to be defined.

Type I IFNs are cellular factors that are critical for the host innate immune response against most viral infections. Therefore, understanding the precise mechanism of the signal transduction events contributing to the establishment of this defense system will have a great impact on the field of viral immunology and infectious diseases. More importantly, research on the SPL–IKKε–IFN axis could extend our knowledge of virus–host interactions and immunoregulatory pathways, which also has translational potential for designing new therapeutic interventions for the treatment of viral infections.

Acknowledgments

We thank Julie Saba (Children's Hospital Oakland Research Institute) for the kind provision of SPL plasmids and David Pintel (University of Missouri) for providing the pCMV-HA plasmid. We also thank Greg Lambert and Michael Baldwin (University of Missouri) for help with confocal microscopy.

Disclosures

The authors have no financial conflicts of interest.

References

1. Seo, Y. J., and B. Hahm. 2010. Type I interferon modulates the battle of host immune system against viruses. *Adv. Appl. Microbiol.* 73: 83–101.
2. Hoffmann, H. H., W. M. Schneider, and C. M. Rice. 2015. Interferons and viruses: an evolutionary arms race of molecular interactions. *Trends Immunol.* 36: 124–138.
3. Isaacs, A., and J. Lindenmann. 2009. Virus interference. I. The interferon. *J. Interferon Res.* 7: 429–438.
4. Katze, M. G., Y. He, and M. Gale, Jr. 2002. Viruses and interferon: a fight for supremacy. *Nat. Rev. Immunol.* 2: 675–687.
5. Goubau, D., S. Deddouche, and C. Reis e Sousa. 2013. Cytosolic sensing of viruses. *Immunity* 38: 855–869.
6. Killip, M. J., E. Fodor, and R. E. Randall. 2015. Influenza virus activation of the interferon system. *Virus Res.* 209: 11–22.
7. Loo, Y. M., J. Fornek, N. Crochet, G. Bajwa, O. Perwitasari, L. Martinez-Sobrido, S. Akira, M. A. Gill, A. García-Sastre, M. G. Katze, and M. Gale, Jr. 2008. Distinct RIG-I and MDA5 signaling by RNA viruses in innate immunity. *J. Virol.* 82: 335–345.
8. Sharma, S., B. R. tenOever, N. Grandvaux, G. P. Zhou, R. Lin, and J. Hiscott. 2003. Triggering the interferon antiviral response through an IKK-related pathway. *Science* 300: 1148–1151.
9. Sato, M., H. Suemori, N. Hata, M. Asagiri, K. Ogasawara, K. Nakao, T. Nakaya, M. Katsuki, S. Noguchi, N. Tanaka, and T. Taniguchi. 2000. Distinct and essential roles of transcription factors IRF-3 and IRF-7 in response to viruses for IFN-alpha/beta gene induction. *Immunity* 13: 539–548.
10. Aaronson, D. S., and C. M. Horvath. 2002. A road map for those who don't know JAK-STAT. *Science* 296: 1653–1655.
11. Schoggins, J. W. 2014. Interferon-stimulated genes: roles in viral pathogenesis. *Curr. Opin. Virol.* 6: 40–46.
12. Beachboard, D. C., and S. M. Horner. 2016. Innate immune evasion strategies of DNA and RNA viruses. *Curr. Opin. Microbiol.* 32: 113–119.
13. Gale Jr., M., and G. C. Sen. 2009. Viral evasion of the interferon system. *J. Interferon Cytokine Res.* 29: 475–476.
14. Aguilar, A., and J. D. Saba. 2012. Truth and consequences of sphingosine-1-phosphate lyase. *Adv. Biol. Regul.* 52: 17–30.
15. Bourquin, F., H. Riezman, G. Capitani, and M. G. Grütter. 2010. Structure and function of sphingosine-1-phosphate lyase, a key enzyme of sphingolipid metabolism. *Structure* 18: 1054–1065.
16. Rolando, M., P. Escoll, and C. Buchrieser. 2016. *Legionella pneumophila* restrains autophagy by modulating the host's sphingolipid metabolism. *Autophagy* 12: 1053–1054.
17. Ikeda, M., A. Kihara, and Y. Igarashi. 2004. Sphingosine-1-phosphate lyase SPL is an endoplasmic reticulum-resident, integral membrane protein with the pyridoxal 5′-phosphate binding domain exposed to the cytosol. *Biochem. Biophys. Res. Commun.* 325: 338–343.
18. Kunkel, G. T., M. Maceyka, S. Milstien, and S. Spiegel. 2013. Targeting the sphingosine-1-phosphate axis in cancer, inflammation and beyond. *Nat. Rev. Drug Discov.* 12: 688–702.
19. Rosen, H., R. C. Stevens, M. Hanson, E. Roberts, and M. B. Oldstone. 2013. Sphingosine-1-phosphate and its receptors: structure, signaling, and influence. *Annu. Rev. Biochem.* 82: 637–662.
20. Newton, J., S. Lima, M. Maceyka, and S. Spiegel. 2015. Revisiting the sphingolipid rheostat: evolving concepts in cancer therapy. *Exp. Cell Res.* 333: 195–200.
21. Fyrst, H., and J. D. Saba. 2008. Sphingosine-1-phosphate lyase in development and disease: sphingolipid metabolism takes flight. *Biochim. Biophys. Acta* 1781: 448–458.

22. Bandhuvula, P., and J. D. Saba. 2007. Sphingosine-1-phosphate lyase in immunity and cancer: silencing the siren. *Trends Mol. Med.* 13: 210–217.
23. Min, J., P. P. Van Veldhoven, L. Zhang, M. H. Hanigan, H. Alexander, and S. Alexander. 2005. Sphingosine-1-phosphate lyase regulates sensitivity of human cells to select chemotherapy drugs in a p38-dependent manner. *Mol. Cancer Res.* 3: 287–296.
24. Li, G., C. Foote, S. Alexander, and H. Alexander. 2001. Sphingosine-1-phosphate lyase has a central role in the development of *Dictyostelium discoideum*. *Development* 128: 3473–3483.
25. Kumar, A., D. Wessels, K. J. Daniels, H. Alexander, S. Alexander, and D. R. Soll. 2004. Sphingosine-1-phosphate plays a role in the suppression of lateral pseudopod formation during *Dictyostelium discoideum* cell migration and chemotaxis. *Cell Motil. Cytoskeleton* 59: 227–241.
26. Herr, D. R., H. Fyrst, V. Phan, K. Heinecke, R. Georges, G. L. Harris, and J. D. Saba. 2003. Sply regulation of sphingolipid signaling molecules is essential for *Drosophila* development. *Development* 130: 2443–2453.
27. Seo, Y. J., C. Blake, S. Alexander, and B. Hahm. 2010. Sphingosine 1-phosphate-metabolizing enzymes control influenza virus propagation and viral cytopathogenicity. *J. Virol.* 84: 8124–8131.
28. Seo, Y. J., S. Alexander, and B. Hahm. 2011. Does cytokine signaling link sphingolipid metabolism to host defense and immunity against virus infections? *Cytokine Growth Factor Rev.* 22: 55–61.
29. Seo, Y. J., C. J. Pritzl, M. Vijayan, K. Bomb, M. E. McClain, S. Alexander, and B. Hahm. 2013. Sphingosine kinase 1 serves as a pro-viral factor by regulating viral RNA synthesis and nuclear export of viral ribonucleoprotein complex upon influenza virus infection. *PLoS One* 8: e75005.
30. Xia, C., M. Vijayan, C. J. Pritzl, S. Y. Fuchs, A. B. McDermott, and B. Hahm. 2015. Hemagglutinin of influenza A virus antagonizes type I interferon (IFN) responses by inducing degradation of type I IFN receptor 1. *J. Virol.* 90: 2403–2417.
31. Reiss, U., B. Oskouian, J. Zhou, V. Gupta, P. Sooriyakumaran, S. Kelly, E. Wang, A. H. Merrill, Jr., and J. D. Saba. 2004. Sphingosine-phosphate lyase enhances stress-induced ceramide generation and apoptosis. *J. Biol. Chem.* 279: 1281–1290.
32. Nakhaei, P., T. Mesplede, M. Solis, Q. Sun, T. Zhao, L. Yang, T. H. Chuang, C. F. Ware, R. Lin, J. Hiscott, and J. Hiscott. 2009. The E3 ubiquitin ligase Triad3A negatively regulates the RIG-I/MAVS signaling pathway by targeting TRAF3 for degradation. *PLoS Pathog.* 5: e1000650.
33. Ran, F. A., P. D. Hsu, J. Wright, V. Agarwala, D. A. Scott, and F. Zhang. 2013. Genome engineering using the CRISPR-Cas9 system. *Nat. Protoc.* 8: 2281–2308.
34. Vijayan, M., Y. J. Seo, C. J. Pritzl, S. A. Squires, S. Alexander, and B. Hahm. 2014. Sphingosine kinase 1 regulates measles virus replication. *Virology* 450-451: 55–63.
35. Vijayan, M., and B. Hahm. 2014. Influenza viral manipulation of sphingolipid metabolism and signaling to modulate host defense system. *Scientifica (Cairo)* 2014: 793815.
36. Kato, H., S. Sato, M. Yoneyama, M. Yamamoto, S. Uematsu, K. Matsui, T. Tsujimura, K. Takeda, T. Fujita, O. Takeuchi, and S. Akira. 2005. Cell type-specific involvement of RIG-I in antiviral response. *Immunity* 23: 19–28.
37. Pichlmair, A., C. Lassnig, C.-A. Eberle, M. W. Górna, C. L. Baumann, T. R. Burkard, T. Bürckstümmer, A. Stefanovic, S. Krieger, K. L. Bennett, et al. 2011. IFIT1 is an antiviral protein that recognizes 5′-triphosphate RNA. *Nat. Immunol.* 12: 624–630.
38. Varga, Z. T., I. Ramos, R. Hai, M. Schmolke, A. García-Sastre, A. Fernandez-Sesma, and P. Palese. 2011. The influenza virus protein PB1-F2 inhibits the induction of type I interferon at the level of the MAVS adaptor protein. *PLoS Pathog.* 7: e1002067.
39. Wang, X., M. Li, H. Zheng, T. Muster, P. Palese, A. A. Beg, and A. García-Sastre. 2000. Influenza A virus NS1 protein prevents activation of NF-kappaB and induction of alpha/beta interferon. *J. Virol.* 74: 11566–11573.
40. Gack, M. U., R. A. Albrecht, T. Urano, K. S. Inn, I. C. Huang, E. Carnero, M. Farzan, S. Inoue, J. U. Jung, and A. García-Sastre. 2009. Influenza A virus NS1 targets the ubiquitin ligase TRIM25 to evade recognition by the host viral RNA sensor RIG-I. *Cell Host Microbe* 5: 439–449.
41. Riegger, D., R. Hai, D. Dornfeld, B. Mänz, V. Leyva-Grado, M. T. Sánchez-Aparicio, R. A. Albrecht, P. Palese, O. Haller, M. Schwemmle, et al. 2015. The nucleoprotein of newly emerged H7N9 influenza A virus harbors a unique motif conferring resistance to antiviral human MxA. *J. Virol.* 89: 2241–2252.
42. Liedmann, S., E. R. Hrincius, C. Guy, D. Anhlan, R. Dierkes, R. Carter, G. Wu, P. Staeheli, D. R. Green, T. Wolff, et al. 2014. Viral suppressors of the RIG-I–mediated interferon response are pre-packaged in influenza virions. *Nat. Commun.* 5: 5645.
43. Graef, K. M., F. T. Vreede, Y. F. Lau, A. W. McCall, S. M. Carr, K. Subbarao, and E. Fodor. 2010. The PB2 subunit of the influenza virus RNA polymerase affects virulence by interacting with the mitochondrial antiviral signaling protein and inhibiting expression of beta interferon. *J. Virol.* 84: 8433–8445.
44. Li, W., H. Chen, T. Sutton, A. Obadan, and D. R. Perez. 2014. Interactions between the influenza A virus RNA polymerase components and retinoic acid-inducible gene I. *J. Virol.* 88: 10432–10447.
45. Goubau, D., M. Schlee, S. Deddouche, A. J. Pruijssers, T. Zillinger, M. Goldeck, C. Schuberth, A. G. Van der Veen, T. Fujimura, J. Rehwinkel, et al. 2014. Antiviral immunity via RIG-I–mediated recognition of RNA bearing 5′-diphosphates. *Nature* 514: 372–375.
46. Shimada, T., T. Kawai, K. Takeda, M. Matsumoto, J. Inoue, Y. Tatsumi, A. Kanamaru, and S. Akira. 1999. IKK-i, a novel lipopolysaccharide-inducible kinase that is related to IkappaB kinases. *Int. Immunol* 11: 1357–1362.
47. Hemmi, H., O. Takeuchi, S. Sato, M. Yamamoto, T. Kaisho, H. Sanjo, T. Kawai, K. Hoshino, K. Takeda, and S. Akira. 2004. The roles of two IkappaB kinase-related kinases in lipopolysaccharide and double stranded RNA signaling and viral infection. *J. Exp. Med.* 199: 1641–1650.
48. Rajsbaum, R., G. A. Versteeg, S. Schmid, A. M. Maestre, A. Belicha-Villanueva, C. Martínez-Romero, J. R. Patel, J. Morrison, G. Pisanelli, L. Miorin, et al. 2014. Unanchored K48-linked polyubiquitin synthesized by the E3-ubiquitin ligase TRIM6 stimulates the interferon-IKKε kinase-mediated antiviral response. *Immunity* 40: 880–895.
49. García-Sastre, A. 2011. Induction and evasion of type I interferon responses by influenza viruses. *Virus Res.* 162: 12–18.
50. van de Sandt, C. E., J. H. Kreijtz, and G. F. Rimmelzwaan. 2012. Evasion of influenza A viruses from innate and adaptive immune responses. *Viruses* 4: 1438–1476.
51. Tenoever, B. R., S. L. Ng, M. A. Chua, S. M. McWhirter, A. García-Sastre, and T. Maniatis. 2007. Multiple functions of the IKK-related kinase IKKepsilon in interferon-mediated antiviral immunity. *Science* 315: 1274–1278.
52. Indukuri, H., S. M. Castro, S.-M. Liao, L. A. Feeney, M. Dorsch, A. J. Coyle, R. P. Garofalo, A. R. Brasier, and A. Casola. 2006. Ikkepsilon regulates viral-induced interferon regulatory factor-3 activation via a redox-sensitive pathway. *Virology* 353: 155–165.
53. tenOever, B. R., S. Sharma, W. Zou, Q. Sun, N. Grandvaux, I. Julkunen, H. Hemmi, M. Yamamoto, S. Akira, W. C. Yeh, et al. 2004. Activation of TBK1 and IKKε kinases by vesicular stomatitis virus infection and the role of viral ribonucleoprotein in the development of interferon antiviral immunity. *J. Virol.* 78: 10636–10649.
54. Prins, K. C., W. B. Cárdenas, and C. F. Basler. 2009. Ebola virus protein VP35 impairs the function of interferon regulatory factor-activating kinases IKKepsilon and TBK-1. *J. Virol.* 83: 3069–3077.
55. Pythoud, C., W. W. Rodrigo, G. Pasqual, S. Rothenberger, L. Martínez-Sobrido, J. C. de la Torre, and S. Kunz. 2012. Arenavirus nucleoprotein targets interferon regulatory factor-activating kinase IKKε. *J. Virol.* 86: 7728–7738.
56. Marsolais, D., B. Hahm, K. B. Walsh, K. H. Edelmann, D. McGavern, Y. Hatta, Y. Kawaoka, H. Rosen, and M. B. Oldstone. 2009. A critical role for the sphingosine analog AAL-R in dampening the cytokine response during influenza virus infection. *Proc. Natl. Acad. Sci. USA* 106: 1560–1565.
57. Teijaro, J. R., K. B. Walsh, S. Cahalan, D. M. Fremgen, E. Roberts, F. Scott, E. Martinborough, R. Peach, M. B. Oldstone, and H. Rosen. 2011. Endothelial cells are central orchestrators of cytokine amplification during influenza virus infection. *Cell* 146: 980–991.
58. Walsh, K. B., J. R. Teijaro, P. R. Wilker, A. Jatzek, D. M. Fremgen, S. C. Das, T. Watanabe, M. Hatta, K. Shinya, M. Suresh, et al. 2011. Suppression of cytokine storm with a sphingosine analog provides protection against pathogenic influenza virus. *Proc. Natl. Acad. Sci. USA* 108: 12018–12023.
59. Marsolais, D., B. Hahm, K. H. Edelmann, K. B. Walsh, M. Guerrero, Y. Hatta, Y. Kawaoka, E. Roberts, M. B. Oldstone, and H. Rosen. 2008. Local not systemic modulation of dendritic cell S1P receptors in lung blunts virus-specific immune responses to influenza. *Mol. Pharmacol.* 74: 896–903.
60. Teijaro, J. R., S. Studer, N. Leaf, W. B. Kiosses, N. Nguyen, K. Matsuki, H. Negishi, T. Taniguchi, M. B. Oldstone, and H. Rosen. 2016. S1PR1-mediated IFNAR1 degradation modulates plasmacytoid dendritic cell interferon-α autoamplification. *Proc. Natl. Acad. Sci. USA* 113: 1351–1356.
61. Degagné, E., and J. D. Saba. 2014. S1pping fire: sphingosine-1-phosphate signaling as an emerging target in inflammatory bowel disease and colitis-associated cancer. *Clin. Exp. Gastroenterol.* 7: 205–214.
62. Nagahashi, M., N. C. Hait, M. Maceyka, D. Avni, K. Takabe, S. Milstien, and S. Spiegel. 2014. Sphingosine-1-phosphate in chronic intestinal inflammation and cancer. *Adv. Biol. Regul.* 54: 112–120.
63. Gonzalez-Cabrera, P. J., S. Brown, S. M. Studer, and H. Rosen. 2014. S1P signaling: new therapies and opportunities. *F1000Prime Rep.* 6: 109.
64. Allende, M. L., M. Bektas, B. G. Lee, E. Bonifacino, J. Kang, G. Tuymetova, W. Chen, J. D. Saba, and R. L. Proia. 2011. Sphingosine-1-phosphate lyase deficiency produces a pro-inflammatory response while impairing neutrophil trafficking. *J. Biol. Chem.* 286: 7348–7358.
65. Zamora-Pineda, J., A. Kumar, J. H. Suh, M. Zhang, and J. D. Saba. 2016. Dendritic cell sphingosine-1-phosphate lyase regulates thymic egress. *J. Exp. Med.* 213: 2773–2791.